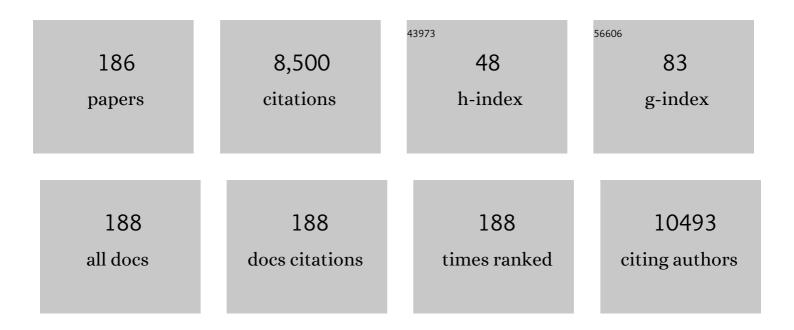


List of Publications by Year in descending order

Source: https://exaly.com/author-pdf/5556083/publications.pdf Version: 2024-02-01



\<u>\</u>/FI\\/FI

#	Article	IF	CITATIONS
1	One‣tep Solvothermal Synthesis of a Carbon@TiO ₂ Dyade Structure Effectively Promoting Visibleâ€Light Photocatalysis. Advanced Materials, 2010, 22, 3317-3321.	11.1	444
2	Novel p–n heterojunction photocatalyst constructed by porous graphite-like C3N4 and nanostructured BiOI: facile synthesis and enhanced photocatalytic activity. Dalton Transactions, 2013, 42, 15726.	1.6	333
3	Enhanced photocatalytic activity over flower-like sphere Ag/Ag2CO3/BiVO4 plasmonic heterojunction photocatalyst for tetracycline degradation. Chemical Engineering Journal, 2018, 331, 242-254.	6.6	285
4	Modifiers-assisted formation of nickel nanoparticles and their catalytic application to p-nitrophenol reduction. CrystEngComm, 2013, 15, 560-569.	1.3	244
5	Constructing graphite-like carbon nitride modified hierarchical yolk–shell TiO ₂ spheres for water pollution treatment and hydrogen production. Journal of Materials Chemistry A, 2016, 4, 1806-1818.	5.2	228
6	Graphitic carbon nitride with different dimensionalities for energy and environmental applications. Nano Research, 2020, 13, 18-37.	5.8	214
7	Ag ₂ S/g-C ₃ N ₄ composite photocatalysts for efficient Pt-free hydrogen production. The co-catalyst function of Ag/Ag ₂ S formed by simultaneous photodeposition. Dalton Transactions, 2014, 43, 4878-4885.	1.6	203
8	Nature-based catalyst for visible-light-driven photocatalytic CO ₂ reduction. Energy and Environmental Science, 2018, 11, 2382-2389.	15.6	198
9	Carbon Dioxide Capture on Amineâ€Rich Carbonaceous Materials Derived from Glucose. ChemSusChem, 2010, 3, 840-845.	3.6	170
10	A new visible light active multifunctional ternary composite based on TiO2–In2O3 nanocrystals heterojunction decorated porous graphitic carbon nitride for photocatalytic treatment of hazardous pollutant and H2 evolution. Applied Catalysis B: Environmental, 2015, 170-171, 195-205.	10.8	160
11	Construction of novel CNT/LaVO4 nanostructures for efficient antibiotic photodegradation. Chemical Engineering Journal, 2019, 357, 487-497.	6.6	158
12	Silver-loaded nitrogen-doped yolk–shell mesoporous TiO ₂ hollow microspheres with enhanced visible light photocatalytic activity. Nanoscale, 2015, 7, 784-797.	2.8	157
13	Removal of cationic dyes from aqueous solution by adsorption onto hydrophobic/hydrophilic silica aerogel. Colloids and Surfaces A: Physicochemical and Engineering Aspects, 2016, 509, 539-549.	2.3	150
14	Highly efficient heterojunction photocatalyst based on nanoporous g-C3N4 sheets modified by Ag3PO4 nanoparticles: Synthesis and enhanced photocatalytic activity. Journal of Colloid and Interface Science, 2014, 417, 115-120.	5.0	143
15	Carbon nitride coupled with CdS-TiO 2 nanodots as 2D/0D ternary composite with enhanced photocatalytic H 2 evolution: A novel efficient three-level electron transfer process. Applied Catalysis B: Environmental, 2017, 210, 194-204.	10.8	133
16	Preparation and characterization of monodisperse Ce-doped TiO2 microspheres with visible light photocatalytic activity. Colloids and Surfaces A: Physicochemical and Engineering Aspects, 2010, 372, 107-114.	2.3	124
17	Facile route fabrication of nano-Ni core mesoporous-silica shell particles with high catalytic activity towards 4-nitrophenol reduction. CrystEngComm, 2012, 14, 4601.	1.3	109
18	MoC–graphite composite as a Pt electrocatalyst support for highly active methanol oxidation and oxygen reduction reaction. Journal of Materials Chemistry A, 2014, 2, 4014.	5.2	106

Wei Wei

#	Article	IF	CITATIONS
19	In situ growth of M-MO (MÂ= Ni, Co) in 3D graphene as a competent bifunctional electrocatalyst for OER and HER. Electrochimica Acta, 2019, 298, 163-171.	2.6	104
20	One-step synthesis of Fe-doped surface-alkalinized g-C3N4 and their improved visible-light photocatalytic performance. Applied Surface Science, 2019, 469, 739-746.	3.1	103
21	Pt supported on Mo2C particles with synergistic effect and strong interaction force for methanol electro-oxidation. Electrochimica Acta, 2013, 95, 218-224.	2.6	92
22	Direct Z-scheme red carbon nitride/rod-like lanthanum vanadate composites with enhanced photodegradation of antibiotic contaminants. Applied Catalysis B: Environmental, 2020, 277, 119245.	10.8	90
23	Constructing polyurethane sponge modified with silica/graphene oxide nanohybrids as a ternary sorbent. Chemical Engineering Journal, 2016, 284, 478-486.	6.6	86
24	In situ synthesis of silver supported nanoporous iron oxide microbox hybrids from metal–organic frameworks and their catalytic application in p-nitrophenol reduction. Physical Chemistry Chemical Physics, 2015, 17, 2550-2559.	1.3	76
25	Efficient Coupling of Nanoparticles to Electrochemically Exfoliated Graphene. Journal of the American Chemical Society, 2015, 137, 5576-5581.	6.6	75
26	A novel Z-scheme CeO2/g-C3N4 heterojunction photocatalyst for degradation of Bisphenol A and hydrogen evolution and insight of the photocatalysis mechanism. Journal of Materials Science and Technology, 2021, 85, 18-29.	5.6	75
27	Synthetic core–shell Ni@Pd nanoparticles supported on graphene and used as an advanced nanoelectrocatalyst for methanol oxidation. New Journal of Chemistry, 2012, 36, 2533.	1.4	74
28	Bamboo leaf-assisted formation of carbon/nitrogen co-doped anatase TiO ₂ modified with silver and graphitic carbon nitride: novel and green synthesis and cooperative photocatalytic activity. Dalton Transactions, 2014, 43, 13792.	1.6	70
29	Natural leaves-assisted synthesis of nitrogen-doped, carbon-rich nanodots-sensitized, Ag-loaded anatase TiO2 square nanosheets with dominant {001} facets and their enhanced catalytic applications. Journal of Materials Chemistry A, 2013, 1, 14963.	5.2	69
30	Enhanced adsorption of hydroxyl contained/anionic dyes on non functionalized Ni@SiO2 core–shell nanoparticles: Kinetic and thermodynamic profile. Applied Surface Science, 2014, 292, 301-310.	3.1	64
31	In situ synthesis of bimetallic Ag/Pt loaded single-crystalline anatase TiO2 hollow nano-hemispheres and their improved photocatalytic properties. CrystEngComm, 2014, 16, 2384.	1.3	64
32	Nitrogen/sulfur co-doped graphene networks uniformly coupled N-Fe2O3 nanoparticles achieving enhanced supercapacitor performance. Electrochimica Acta, 2018, 266, 242-253.	2.6	63
33	Carbon nitride nanowires/nanofibers: A novel template-free synthesis from a cyanuric chloride–melamine precursor towards enhanced adsorption and visible-light photocatalytic performance. Ceramics International, 2016, 42, 4158-4170.	2.3	62
34	In situ chemical transformation synthesis of Bi ₄ Ti ₃ O ₁₂ /l–BiOCl 2D/2D heterojunction systems for water pollution treatment and hydrogen production. Catalysis Science and Technology, 2017, 7, 3863-3875.	2.1	62
35	In situ construction efficient visible-light-driven three-dimensional Polypyrrole/Zn3In2S6 nanoflower to systematically explore the photoreduction of Cr(VI): Performance, factors and mechanism. Journal of Hazardous Materials, 2020, 384, 121480.	6.5	61
36	Enhanced electrocatalytic activity of high Pt-loadings on surface functionalized graphene nanosheets for methanol oxidation. International Journal of Hydrogen Energy, 2013, 38, 16402-16409.	3.8	58

#	Article	IF	CITATIONS
37	M _X P(M = Co/Ni)@carbon core–shell nanoparticles embedded in 3D cross-linked graphene aerogel derived from seaweed biomass for hydrogen evolution reaction. Nanoscale, 2018, 10, 9698-9706.	2.8	58
38	Characterization and comparison of uniform hydrophilic/hydrophobic transparent silica aerogel beads: skeleton strength and surface modification. RSC Advances, 2015, 5, 55579-55587.	1.7	56
39	A bimetallic carbide Fe2MoC promoted Pd electrocatalyst with performance superior to Pt/C towards the oxygen reduction reaction in acidic media. Applied Catalysis B: Environmental, 2015, 165, 636-641.	10.8	56
40	Freeze–Thawâ€Promoted Fabrication of Clean and Hierarchically Structured Nobleâ€Metal Aerogels for Electrocatalysis and Photoelectrocatalysis. Angewandte Chemie - International Edition, 2020, 59, 8293-8300.	7.2	56
41	Graphene Nanosphere as Advanced Electrode Material to Promote High Performance Symmetrical Supercapacitor. Small, 2021, 17, e2007915.	5.2	56
42	Graphite-like carbon nitride coupled with tiny Bi2S3 nanoparticles as 2D/0D heterojunction with enhanced photocatalytic activity. Applied Surface Science, 2018, 444, 75-86.	3.1	55
43	Ternary MIL-100(Fe)@Fe3O4/CA magnetic nanophotocatalysts (MNPCs): Magnetically separable and Fenton-like degradation of tetracycline hydrochloride. Advanced Powder Technology, 2018, 29, 3305-3314.	2.0	55
44	Cobalt phosphide nanoparticles embedded in 3D N-doped porous carbon for efficient hydrogen and oxygen evolution reactions. International Journal of Hydrogen Energy, 2019, 44, 4543-4552.	3.8	52
45	MoO2 nanocrystals down to 5Ânm as Pt electrocatalyst promoter for stable oxygen reduction reaction. International Journal of Hydrogen Energy, 2012, 37, 15948-15955.	3.8	51
46	Facile synthesis silver nanoparticles on different xerogel supports as highly efficient catalysts for the reduction of p-nitrophenol. Colloids and Surfaces A: Physicochemical and Engineering Aspects, 2017, 520, 743-756.	2.3	51
47	Photocatalytic reduction of CO2 and degradation of Bisphenol-S by g-C3N4/Cu2O@Cu S-scheme heterojunction: Study on the photocatalytic performance and mechanism insight. Carbon, 2022, 193, 272-284.	5.4	51
48	Graphene-analogue BN-modified microspherical BiOI photocatalysts driven by visible light. Dalton Transactions, 2016, 45, 2505-2516.	1.6	50
49	Synthesis and characterization of superhydrophobic silica and silica/titania aerogels by sol–gel method at ambient pressure. Colloids and Surfaces A: Physicochemical and Engineering Aspects, 2009, 342, 97-101.	2.3	49
50	Electrochemical CO2 reduction on copper nanoparticles-dispersed carbon aerogels. Journal of Colloid and Interface Science, 2019, 545, 1-7.	5.0	48
51	Integrating CoOx cocatalyst on hexagonal α-Fe2O3 for effective photocatalytic oxygen evolution. Applied Surface Science, 2019, 469, 933-940.	3.1	48
52	Cobalt encapsulated N-doped defect-rich carbon nanotube as pH universal hydrogen evolution electrocatalyst. Applied Surface Science, 2018, 446, 10-17.	3.1	47
53	CoP nanoparticles encapsulated in three-dimensional N-doped porous carbon for efficient hydrogen evolution reaction in a broad pH range. Applied Surface Science, 2019, 476, 749-756.	3.1	47
54	In situ growth of N-doped carbon coated CoNi alloy with graphene decoration for enhanced HER performance. Journal of Energy Chemistry, 2019, 29, 129-135.	7.1	47

#	Article	IF	CITATIONS
55	Self-assembling NiCo2S4 nanorods arrays and T-Nb2O5 nanosheets/three-dimensional nitrogen-doped garphene hybrid nanoarchitectures for advanced asymmetric supercapacitor. Chemical Engineering Journal, 2020, 392, 123669.	6.6	47
56	Ni3Fe nanoparticles enclosed by B-doped carbon for efficient bifunctional performances of oxygen and hydrogen evolution reactions. Journal of Alloys and Compounds, 2020, 835, 155267.	2.8	46
57	A facile strategy for SnS2/g-C3N4 heterojunction composite and the mechanism in photocatalytic degradation of MO. Journal of Molecular Catalysis A, 2016, 425, 174-182.	4.8	45
58	Gentle way to build reduced titanium dioxide nanodots integrated with graphite-like carbon spheres: From DFT calculation to experimental measurement. Applied Catalysis B: Environmental, 2017, 204, 283-295.	10.8	45
59	Robust bifunctional catalytic activities of N-doped carbon aerogel-nickel composites for electrocatalytic hydrogen evolution and hydrogenation of nitrocompounds. International Journal of Hydrogen Energy, 2019, 44, 13334-13344.	3.8	45
60	Biomass-derived multifunctional TiO ₂ /carbonaceous aerogel composite as a highly efficient photocatalyst. RSC Advances, 2016, 6, 25255-25266.	1.7	44
61	Uniform Cu2Cl(OH)3 hierarchical microspheres: A novel adsorbent for methylene blue adsorptive removal from aqueous solution. Journal of Solid State Chemistry, 2013, 204, 305-313.	1.4	43
62	Smaller Pt particles supported on mesoporous bowl-like carbon for highly efficient and stable methanol oxidation and oxygen reduction reaction. Journal of Power Sources, 2013, 243, 48-53.	4.0	43
63	Improved catalytic activity of cobalt core–platinum shell nanoparticles supported on surface functionalized graphene for methanol electro-oxidation. Electrochimica Acta, 2015, 158, 81-88.	2.6	43
64	Novel one-step synthesis of nickel encapsulated carbon nanotubes as efficient electrocatalyst for hydrogen evolution reaction. International Journal of Hydrogen Energy, 2019, 44, 2685-2693.	3.8	43
65	Nickel-based xerogel catalysts: Synthesis via fast sol-gel method and application in catalytic hydrogenation of p -nitrophenol to p -aminophenol. Applied Surface Science, 2016, 382, 135-143.	3.1	42
66	Brookite titania photocatalytic nanomaterials: Synthesis, properties, and applications. Pure and Applied Chemistry, 2009, 81, 2407-2415.	0.9	40
67	Fabrication of Ag/AgCl/ZnFe2O4 composites with enhanced photocatalytic activity for pollutant degradation and E. coli disinfection. Colloids and Surfaces A: Physicochemical and Engineering Aspects, 2018, 553, 114-124.	2.3	40
68	Nickel and cobalt in situ grown in 3-dimensional hierarchical porous graphene for effective methanol electro-oxidation reaction. Journal of Electroanalytical Chemistry, 2019, 838, 7-15.	1.9	40
69	Natural carbon nanodots assisted development of size-tunable metal (Pd, Ag) nanoparticles grafted on bionic dendritic α-Fe ₂ O ₃ for cooperative catalytic applications. Journal of Materials Chemistry A, 2015, 3, 23607-23620.	5.2	39
70	Nitrogen doped lotus stem carbon as electrocatalyst comparable to Pt/C for oxygen reduction reaction in alkaline media. International Journal of Hydrogen Energy, 2017, 42, 20560-20567.	3.8	39
71	Chrysanthemum-like FeS/Ni3S2 heterostructure nanoarray as a robust bifunctional electrocatalyst for overall water splitting. Journal of Colloid and Interface Science, 2022, 608, 536-548.	5.0	39
72	An ion exchange route to produce WO3 nanobars as Pt electrocatalyst promoter for oxygen reduction reaction. Journal of Power Sources, 2013, 222, 218-224.	4.0	36

#	Article	IF	CITATIONS
73	Integrating AgI/AgBr biphasic heterostructures encased by few layer h-BN with enhanced catalytic activity and stability. Journal of Colloid and Interface Science, 2017, 496, 434-445.	5.0	36
74	Novel broad-spectrum-driven oxygen-linked band and porous defect co-modified orange carbon nitride for photodegradation of Bisphenol A and 2-Mercaptobenzothiazole. Journal of Hazardous Materials, 2020, 396, 122659.	6.5	36
75	Highly efficient visible-light photocatalysts: reduced graphene oxide and C ₃ N ₄ nanosheets loaded with Ag nanoparticles. RSC Advances, 2015, 5, 15993-15999.	1.7	35
76	Ag ₂ S quantum dots in situ coupled to hexagonal SnS ₂ with enhanced photocatalytic activity for MO and Cr(<scp>vi</scp>) removal. RSC Advances, 2017, 7, 46823-46831.	1.7	35
77	Cobalt–Iron nanoparticles encapsulated in mesoporous carbon nanosheets: A one-pot synthesis of highly stable electrocatalysts for overall water splitting. International Journal of Hydrogen Energy, 2021, 46, 5234-5249.	3.8	35
78	Selective adsorption of organic dyes by porous hydrophilic silica aerogels from aqueous system. Water Science and Technology, 2018, 78, 402-414.	1.2	34
79	Vanadium carbide and graphite promoted Pd electrocatalyst for ethanol oxidation in alkaline media. Journal of Power Sources, 2013, 243, 336-342.	4.0	33
80	Low temperature synthesis of anatase rare earth doped titania-silica photocatalyst and its photocatalytic activity under solar-light. Colloids and Surfaces A: Physicochemical and Engineering Aspects, 2010, 355, 178-182.	2.3	32
81	Hollow molybdenum carbide sphere promoted Pt electrocatalyst for oxygen reduction and methanol oxidation reaction. Journal of Power Sources, 2015, 286, 239-246.	4.0	31
82	Graphene oxide-modified LaVO ₄ nanocomposites with enhanced photocatalytic degradation efficiency of antibiotics. Inorganic Chemistry Frontiers, 2018, 5, 2818-2828.	3.0	31
83	<i>In situ</i> confined vertical growth of a 1D-CuCo ₂ S ₄ nanoarray on Ni foam covered by a 3D-PANI mesh layer to form a self-supporting hierarchical structure for high-efficiency oxygen evolution catalysis. Nanoscale, 2019, 11, 12326-12336.	2.8	31
84	Simplistic two-step fabrication of porous carbon-based biomass-derived electrocatalyst for efficient hydrogen evolution reaction. Energy Conversion and Management, 2021, 227, 113628.	4.4	31
85	Ionic liquid-assisted hydrothermal synthesis of square BiOBr nanoplates with highly efficient photocatalytic activity. Materials Letters, 2014, 118, 154-157.	1.3	30
86	Controllable fabrication of abundant nickel-nitrogen doped CNT electrocatalyst for robust hydrogen evolution reaction. Applied Surface Science, 2021, 562, 150161.	3.1	30
87	Deposition of Ag nanoparticles on g-C ₃ N ₄ nanosheet by <i>N</i> , <i>N</i> -dimethylformamide: Soft synthesis and enhanced photocatalytic activity. Journal of Materials Research, 2014, 29, 2170-2178.	1.2	29
88	A novel route for synthesis of UV-resistant hydrophobic titania-containing silica aerogels by using potassium titanate as precursor. Dalton Transactions, 2014, 43, 9456.	1.6	29
89	Nickel core–palladium shell nanoparticles grown on nitrogen-doped graphene with enhanced electrocatalytic performance for ethanol oxidation. RSC Advances, 2016, 6, 33231-33239.	1.7	29
90	In situ growth of Ag/Ag ₂ O nanoparticles on g-C ₃ N ₄ by a natural carbon nanodot-assisted green method for synergistic photocatalytic activity. RSC Advances, 2016, 6, 3186-3197.	1.7	29

#	Article	IF	CITATIONS
91	Synergistically coupling of Co/Mo2C/Co6Mo6C2@C electrocatalyst for overall water splitting: The role of carbon precursors in structural engineering and catalytic activity. Applied Surface Science, 2022, 579, 152148.	3.1	29
92	Cell wall disruption in low temperature NaOH/urea solution and its potential application in lignocellulose pretreatment. Cellulose, 2015, 22, 3559-3568.	2.4	28
93	A controlled solvethermal approach to synthesize nanocrystalline iron oxide for congo red adsorptive removal from aqueous solutions. Journal of Materials Science, 2016, 51, 4481-4494.	1.7	28
94	Nitrogen doped porous carbon with iron promotion for oxygen reduction reaction in alkaline and acidic media. International Journal of Hydrogen Energy, 2019, 44, 4090-4101.	3.8	28
95	3D graphene decorated with hexagonal micro-coin of Co(OH)2: A competent electrocatalyst for hydrogen and oxygen evolution reaction. International Journal of Hydrogen Energy, 2019, 44, 14770-14779.	3.8	28
96	Small-sized Pt particles on mesoporous hollow carbon spheres for highly stable oxygen reduction reaction. Electrochimica Acta, 2013, 109, 256-261.	2.6	27
97	Comparative study of modified/non-modified aluminum and silica aerogels for anionic dye adsorption performance. RSC Advances, 2018, 8, 29129-29140.	1.7	26
98	Realizing the synergistic effect of electronic modulation over graphitic carbon nitride for highly efficient photodegradation of bisphenol A and 2-mercaptobenzothiazole: Mechanism, degradation pathway and density functional theory calculation. Journal of Colloid and Interface Science, 2021, 583, 113-127.	5.0	26
99	Preparation of cobalt silicide on graphene as Pt electrocatalyst supports for highly efficient and stable methanol oxidation in acidic media. Electrochimica Acta, 2015, 161, 48-54.	2.6	25
100	Mesoporous graphene-like nanobowls as Pt electrocatalyst support for highly active and stable methanol oxidation. Journal of Power Sources, 2015, 284, 497-503.	4.0	24
101	Constructing mesoporous Bi4Ti3O12 with enhanced visible light photocatalytic activity. Materials Letters, 2016, 183, 303-306.	1.3	24
102	Highly efficient photocatalytic degradation of the Tetracycline hydrochloride on the α-Fe2O3@CN composite under the visible light. Journal of Environmental Chemical Engineering, 2019, 7, 103322.	3.3	24
103	Hierarchically grown ZnFe2O4-decorated polyaniline-coupled-graphene nanosheets as a novel electrocatalyst for selective detecting p-nitrophenol. Microchemical Journal, 2021, 160, 105777.	2.3	24
104	Efficient removal of erichrome black T with biomass-derived magnetic carbonaceous aerogel sponge. Materials Science and Engineering B: Solid-State Materials for Advanced Technology, 2019, 248, 114387.	1.7	23
105	Synthesis and studies of ZnO doped with g-C3N4 nanocomposites for the degradation of tetracycline hydrochloride under the visible light irradiation. Journal of Environmental Chemical Engineering, 2019, 7, 103152.	3.3	23
106	Nickel loaded graphene-like carbon sheets an improved electrocatalyst for hydrogen evolution reaction. Materials Chemistry and Physics, 2019, 227, 105-110.	2.0	22
107	Construction of dual ion (Fe3+/Fe2+ and Nb5+/Nb4+) synergy and full spectrum 1D nanorod Fe2O3/NaNbO3 photo-Fenton catalyst for the degradation of antibiotic: Effects of H2O2, S2O82â^' and toxicity. Separation and Purification Technology, 2021, 261, 118269.	3.9	22
108	Fabrication of noble-metal-free NiS2/g-C3N4 hybrid photocatalysts with visible light-responsive photocatalytic activities. Research on Chemical Intermediates, 2016, 42, 6483-6499.	1.3	21

#	Article	IF	CITATIONS
109	Controlled self-assembly synthesis of CuCo2O4/rGO for improving the morphology-dependent electrochemical oxygen evolution performance. Applied Surface Science, 2019, 493, 710-718.	3.1	21
110	Facile Surface Engineering of Ag–In–Zn–S Quantum Dot Photocatalysts by Mixed-Ligand Passivation with Improved Charge Carrier Lifetime. Catalysis Letters, 2019, 149, 1800-1812.	1.4	21
111	Facile synthesis of N, S co-doped MoO2@C nanorods as an outstanding electrocatalyst for hydrogen evolution reaction. Applied Surface Science, 2021, 537, 147971.	3.1	21
112	Nitrogenâ€Doped Bimetallic Carbideâ€Graphite Composite as Highly Active and Extremely Stable Electrocatalyst for Oxygen Reduction Reaction in Alkaline Media. Advanced Functional Materials, 2022, 32, .	7.8	21
113	Construction of Bi 2 Ti 2 O 7 /Bi 4 Ti 3 O 12 composites with enhanced visible light photocatalytic activity. Materials Letters, 2017, 206, 245-248.	1.3	20
114	BiPO4 nanorods anchored in biomass-based carbonaceous aerogel skeleton: A 2D-3D heterojunction composite as an energy-eï¬∫cient photocatalyst. Journal of Supercritical Fluids, 2019, 147, 33-41.	1.6	20
115	Pd supported on 2–4nm MoC particles with reduced particle size, synergistic effect and high stability for ethanol oxidation. Electrochimica Acta, 2013, 108, 644-650.	2.6	19
116	Iron promoted nitrogen doped porous graphite for efficient oxygen reduction reaction in alkaline and acidic media. Journal of Alloys and Compounds, 2019, 773, 819-827.	2.8	19
117	Fabrication of carbon nanotubes encapsulated cobalt phosphide on graphene: Cobalt promoted hydrogen evolution reaction performance. Electrochimica Acta, 2020, 330, 135213.	2.6	19
118	Preparation of magnetically recoverable and Z-scheme BaFe12O19/AgBr composite for degradation of 2-Mercaptobenzothiazole and Methyl orange under visible light. Applied Surface Science, 2020, 521, 146343.	3.1	19
119	Facile synthesis of Ni5P4 nanosheets/nanoparticles for highly active and durable hydrogen evolution. International Journal of Hydrogen Energy, 2021, 46, 11701-11710.	3.8	19
120	Ni/MWCNT-Supported Palladium Nanoparticles as Magnetic Catalysts for Selective Oxidation of Benzyl Alcohol. Australian Journal of Chemistry, 2013, 66, 564.	0.5	18
121	Transforming MoO3 macrorods into bismuth molybdate nanoplates via the surfactant-assisted hydrothermal method. Ceramics International, 2015, 41, 11471-11481.	2.3	18
122	The construction of a Fenton system to achieve in situ H2O2 generation and decomposition for enhanced photocatalytic performance. Inorganic Chemistry Frontiers, 2019, 6, 1490-1500.	3.0	18
123	Incorporation of pyridinic and graphitic N to Ni@ <scp>CNTs</scp> : As a competent electrocatalyst for hydrogen evolution reaction. International Journal of Energy Research, 2020, 44, 9157-9165.	2.2	18
124	Hierarchical Co/MoO2@N-doped carbon nanosheets derived from waste lotus leaves for electrocatalytic water splitting. International Journal of Hydrogen Energy, 2022, 47, 15673-15686.	3.8	18
125	An ultrastable bimetallic carbide as platinum electrocatalyst support for highly active oxygen reduction reaction. Journal of Power Sources, 2015, 295, 156-161.	4.0	17
126	Dispersed copper nanoparticles promote the electron mobility of nitrogen-rich graphitized carbon aerogel for electrochemical determination of 4-nitrophenol. Mikrochimica Acta, 2019, 186, 853.	2.5	17

Wei Wei

#	Article	IF	CITATIONS
127	Hierarchical porous nitrogen-doped graphite from tissue paper as efficient electrode material for symmetric supercapacitor. Journal of Power Sources, 2021, 492, 229670.	4.0	17
128	Ni-Fe-Co based mixed metal/metal-oxides nanoparticles encapsulated in ultrathin carbon nanosheets: A bifunctional electrocatalyst for overall water splitting. Surfaces and Interfaces, 2021, 26, 101361.	1.5	17
129	Preparation and characterization of heterojunction semiconductor YFeO ₃ /TiO ₂ with an enhanced photocatalytic activity. Journal of Materials Research, 2010, 25, 104-109.	1.2	16
130	Tunable synthesis of enhanced photodegradation activity of brookite/anatase mixed-phase titanium dioxide. Journal of Materials Research, 2013, 28, 400-404.	1.2	16
131	In situ formation of small-scale Ag2S nanoparticles in carbonaceous aerogel for enhanced photodegradation performance. Journal of Molecular Liquids, 2019, 292, 111476.	2.3	16
132	B-doped carbon enclosed Ni nanoparticles: A robust, stable and efficient electrocatalyst for hydrogen evolution reaction. Journal of Electroanalytical Chemistry, 2020, 869, 114085.	1.9	16
133	CTAB-assisted synthesis and characterization of Bi2WO6 photocatalysts grown from WO3·0.33H2O nanoplate precursors. Monatshefte Für Chemie, 2014, 145, 47-59.	0.9	15
134	Hollow tungsten carbide/carbon sphere promoted Pt electrocatalyst for efficient methanol oxidation. RSC Advances, 2015, 5, 6790-6796.	1.7	15
135	Use of Carbon Nanotubes as a Solid Support To Establish Quantitative (Centrifugation) and Qualitative (Filtration) Immunoassays To Detect Gentamicin Contamination in Commercial Milk. Journal of Agricultural and Food Chemistry, 2016, 64, 7874-7881.	2.4	15
136	Synthesis, characterization, and adsorption properties of silica aerogels crosslinked with diisocyanate under ambient drying. Journal of Materials Science, 2016, 51, 9472-9483.	1.7	15
137	ZnS@carbonaceous aerogel composites fabricated in production of hydrogen and for removal of organic pollutants. Journal of Materials Science: Materials in Electronics, 2018, 29, 8523-8534.	1.1	15
138	Fabrication of CNTs encapsulated nickel-nickel phosphide nanoparticles on graphene for remarkable hydrogen evolution reaction performance. Journal of Electroanalytical Chemistry, 2019, 846, 113142.	1.9	15
139	Porous, thick nitrogen-doped carbon encapsulated large PtNi core-shell nanoparticles for oxygen reduction reaction with extreme stability and activity. Carbon, 2022, 186, 36-45.	5.4	15
140	Cage-like pores of a metal–organic framework for separations and encapsulation of Pd nanoparticles for efficient catalysis. New Journal of Chemistry, 2015, 39, 2669-2674.	1.4	14
141	Novel 3D graphene ornamented with CoO nanoparticles as an efficient bifunctional electrocatalyst for oxygen and hydrogen evolution reactions. Materials Chemistry and Physics, 2021, 261, 124237.	2.0	14
142	Hydrothermal synthesis and properties of BiVO ₄ photocatalysts. Journal of Materials Research, 2013, 28, 3408-3416.	1.2	13
143	Synthetic bismuth silicate nanostructures: Photocatalysts grown from silica aerogels precursors. Journal of Materials Research, 2013, 28, 1658-1668.	1.2	13
144	Enhancing the photocatalytic performance of g-C3N4 by using iron single-atom doping for the reduction of U(VI) in aqueous solutions. Journal of Solid State Chemistry, 2022, 312, 123160.	1.4	13

#	Article	IF	CITATIONS
145	Novel broad-spectrum-driven g-C3N4 with oxygen-linked band and porous defect for photodegradation of bisphenol A, 2-mercaptophenthiazole and ciprofloxacin. Chemosphere, 2021, 268, 128839.	4.2	12
146	Structures, photoluminescence and heterogeneous catalysis of five metal complexes constructed by a flexible tricarboxylate ligand. Polyhedron, 2014, 81, 32-38.	1.0	11
147	A novel synthesis of P/BiPO ₄ nanocomposites with enhanced visible-light photocatalysis. Materials Research Innovations, 2015, 19, 361-367.	1.0	11
148	Solvothermal engineering of bismuth molybdate with C3N4 nanosheets, and enhanced photocatalytic activity. Research on Chemical Intermediates, 2015, 41, 9629-9642.	1.3	11
149	Controllable synthesis of magnetic Fe3O4 encapsulated semimetal Bi nanospheres with excellent stability and catalytic activity. Journal of Materials Science, 2018, 53, 13886-13899.	1.7	11
150	Tungsten Carbide Synthesized by Polystyrene Sphere Template Method Promoting Pd Electrocatalyst for Alcohol Oxidation in Alkaline Media. Fuel Cells, 2015, 15, 256-261.	1.5	10
151	Isolation and Characterization of Aphidicolin Derivatives from Tolypocladium inflatum. Molecules, 2017, 22, 1168.	1.7	10
152	Facile synthesis of Cu nanoparticles on different morphology ZrO2 supports for catalytic hydrogen generation from ammonia borane. Journal of Materials Science: Materials in Electronics, 2018, 29, 14971-14980.	1.1	9
153	The effect of solvent parameters on properties of iron-based silica binary aerogels as adsorbents. Journal of Colloid and Interface Science, 2019, 549, 189-200.	5.0	9
154	Porous carbonized egg white as efficient electrocatalyst for oxygen reduction reaction. International Journal of Hydrogen Energy, 2021, 46, 21112-21123.	3.8	9
155	NiCoP nanoparticles encapsulated in cross-linked graphene aerogel to efficient hydrogen evolution reaction. Journal of Materials Science: Materials in Electronics, 2020, 31, 13521-13530.	1.1	8
156	Size-controllable synthesis of zinc ferrite/reduced graphene oxide aerogels: efficient electrochemical sensing of p-nitrophenol. Nanotechnology, 2020, 31, 435706.	1.3	8
157	Reduced graphene oxide decorated CoSnO3@ZnSnO3 with multi-component double-layered hollow nanoboxes for high energy storage and capacity retention asymmetric supercapacitors. Journal of Alloys and Compounds, 2021, 857, 157536.	2.8	8
158	Mechanosynthesis of polymer-stabilized lead bromide perovskites: insight into the formation and phase conversion of nanoparticles. Nano Research, 2021, 14, 1078-1086.	5.8	8
159	Highly Stable Ultrafine Boronâ€Doped NiCo@Carbon Nanoparticles as a Robust Electrocatalyst for the Hydrogen Evolution Reaction. ChemElectroChem, 2021, 8, 1337-1348.	1.7	8
160	Angstrom-scale vanadium carbide rods as Pt electrocatalyst support for efficient methanol oxidation reaction. RSC Advances, 2015, 5, 9561-9564.	1.7	7
161	Simultaneous fabrication of cobaltâ€based graphene with rich N dopant for hydrogen evolution reaction in basic medium. International Journal of Energy Research, 2021, 45, 14010-14020.	2.2	7
162	Rational fabrication of chitosan/alginate/silica ternary aerogel beads adsorbent with free separation. Micro and Nano Letters, 2019, 14, 142-145.	0.6	7

#	Article	IF	CITATIONS
163	Reactivity and Mechanistic Insight into Visible-Light-Induced Anerobic Selective Reaction by Ag/Brookite Titania. Journal of Nanoscience and Nanotechnology, 2012, 12, 8017-8022.	0.9	6
164	Angstrom-sized tungsten carbide promoted platinum electrocatalyst for effective oxygen reduction reaction and resource saving. RSC Advances, 2015, 5, 96488-96494.	1.7	6
165	Fabrication of polysiloxane-modified polyurethane sponge as low-cost organics/water separation and selective absorption material. Water Science and Technology, 2016, 74, 1936-1945.	1.2	6
166	Exterior and small carbide particle promoted platinum electrocatalyst for efficient methanol oxidation. RSC Advances, 2016, 6, 66665-66671.	1.7	6
167	Controllable electrostatic manipulation of structure building blocks in noble metal aerogels. Materials Advances, 2022, 3, 5760-5771.	2.6	6
168	UV-resistant hydrophobic rutile titania aerogels synthesized through a nonalkoxide ambient pressure drying process. Journal of Materials Research, 2013, 28, 378-384.	1.2	5
169	Formation of cobalt silicide nanoparticles on graphene with a synergistic effect and high stability for ethanol oxidation. RSC Advances, 2016, 6, 30293-30300.	1.7	5
170	Embedded cobalt sulfide/N-doped reduced graphene oxide nanocomposite for high-efficiency hydrogen evolution catalysis. Materials Research Express, 2019, 6, 115508.	0.8	5
171	Heterogeneous form of poly (4-vinyl pyridine) beads based dendrimer stabilized Ag, Au and PdNPs catalyst for reduction of trypan blue. Materials Science for Energy Technologies, 2019, 2, 532-542.	1.0	5
172	Microwave-assisted synthesis of mesoporous hemispherical graphite promoted with iron and nitrogen doping for reduction of oxygen. Journal of Alloys and Compounds, 2020, 838, 155608.	2.8	5
173	Interrelations between sulfur, iron, nitrogen, pore and graphite matrix for oxygen reduction reaction. International Journal of Hydrogen Energy, 2020, 45, 11321-11329.	3.8	5
174	Novel ionic liquid modified carbon nitride fabricated by in situ pyrolysis of 1-butyl-3-methylimidazolium cyanamide to improve electronic structure for efficiently degradation of bisphenol A. Colloids and Surfaces A: Physicochemical and Engineering Aspects, 2021, 610, 125648.	2.3	5
175	Enzyme-linked immunosorbent assay for triclocarban in aquatic environments. Water Science and Technology, 2015, 72, 1682-1691.	1.2	4
176	Smart strategy to synthesis silverâ€based heterogeneous photocatalysts grown from molybdenum oxide precursor. Micro and Nano Letters, 2017, 12, 978-981.	0.6	4
177	Surface-amino-induced boosting solar conversion of CO2 to CO over natural metal-free catalyst. Journal of CO2 Utilization, 2021, 54, 101773.	3.3	4
178	Catalysts derived from Earth-abundant natural biomass enable efficient photocatalytic CO2 conversion for achieving a closed-loop carbon cycle. Green Chemistry, 2021, 23, 9683-9692.	4.6	4
179	Low Temperature Preparation and Visible Light Induced Photocatalytic Activity of Europium Doped Hydrophobic Anatase TiO ₂ –SiO ₂ Photocatalysts. Journal of Nanoscience and Nanotechnology, 2010, 10, 7663-7666.	0.9	3
180	Application of Hydrophobic Silica/Fiber Composite Aerogels in Organic Absorption. Materials Science Forum, 0, 675-677, 1035-1039.	0.3	3

#	Article	IF	CITATIONS
181	Simultaneous synthesis of bimetallic@3D graphene electrocatalyst for HER and OER. Frontiers of Materials Science, 2021, 15, 305-315.	1.1	3
182	Poly(styrene) Beads Grafted with Dendrimer Stabilized Gold Nanoparticles for Catalytic Reduction of 4-Nitrophenol. Asian Journal of Chemistry, 2019, 31, 235-246.	0.1	2
183	Cu–Co bimetallic nanospheres embedded in graphene as excellent anode catalysts for electrocatalytic oxygen evolution reaction. Micro and Nano Letters, 2019, 14, 466-469.	0.6	2
184	Comparative Study of Alkali and Acidic Cellulose Solvent Pretreatment of Corn Stover for Fermentable Sugar Production. BioResources, 2015, 11, .	0.5	1
185	Solvent Recovery of Silica Aerogel Monoliths Synthesis and Adsorption of Trivalent Chromium Ions. Advanced Materials Research, 2013, 750-752, 1326-1330.	0.3	0
186	Rücktitelbild: Freeze–Thawâ€Promoted Fabrication of Clean and Hierarchically Structured Nobleâ€Metal Aerogels for Electrocatalysis and Photoelectrocatalysis (Angew. Chem. 21/2020). Angewandte Chemie, 2020, 132, 8379-8379.	1.6	0